

Bromine-induced oxidation of mercury in the mid-latitude atmosphere

Daniel Obrist^{1*}, Eran Tas^{2,3}, Mordechai Peleg², Valeri Matveev², Xavier Faïn¹, David Asaf² and Menachem Luria²

Mercury is a potent neurotoxin, which enters remote ecosystems primarily through atmospheric deposition^{1,2}. In the polar atmosphere, gaseous elemental mercury is oxidized to a highly reactive form of mercury, which is rapidly removed from the atmosphere by deposition^{3,4}. These atmospheric mercury-depletion events are caused by reactive halogens, such as bromine, which are released from sea-ice surfaces^{5,6}. Reactive halogens also exist at temperate and low latitudes^{7,8}, but their influence on mercury in the atmosphere outside polar regions has remained uncertain. Here we show that bromine can oxidize gaseous elemental mercury at mid-latitudes, using measurements of atmospheric mercury, bromine oxide and other trace gases over the Dead Sea, Israel. We observed some of the highest concentrations of reactive mercury measured in the Earth's atmosphere. Peaks in reactive mercury concentrations coincided with the near-complete depletion of elemental mercury, suggesting that elemental mercury was the source. The production of reactive mercury generally coincided with high concentrations of bromine oxide, but was also apparent at low levels of bromine oxide, and was observed at temperatures of up to 45 °C. Using a chemical box model, we show that bromine species were the primary oxidants of elemental mercury over the Dead Sea. We suggest that bromine-induced mercury oxidation may be an important source of mercury to the world's oceans.

Atmospheric mercury depletion events (AMDE; ref. 3) have been described in many Arctic, sub-Arctic and Antarctic sites, where they lead to pulses of increased mercury deposition^{9,10} and are estimated to increase mercury loads to the Arctic by 120–300 Mg each year^{11,12}. AMDE are caused by reactive halogens¹³ and accompanied by low levels of ozone (O₃), which is catalytically destroyed by halogens¹⁴. Reactive halogens, however, are not limited to the polar atmosphere and occur at temperate locations such as over salt lakes and in the marine boundary layer^{7,8,15,16}. The degree to which reactive halogens cause conversion of elemental mercury, Hg(0), to oxidized mercury, Hg(II), under non-freezing conditions at temperate and low latitudes is unclear.

We report results from measurements on the shore of the Dead Sea, Israel, where we simultaneously quantified the main forms of atmospheric mercury, Hg(0) and gaseous and particulate-bound Hg(II), bromine oxide (BrO), O₃ and auxiliary variables. We measured atmospheric mercury by means of cold-vapour atomic fluorescence spectrometry and BrO using long-path differential optical absorption spectroscopy (LP-DOAS), and quantified other trace gases (including O₃) and meteorology during two measurement campaigns in summer and winter. Time series

of measurements (Fig. 1a,b) showed daytime Hg(II) enrichment to levels as high as 136 ppqv, among the highest Hg(II) levels observed in the Earth's atmosphere⁴. High daytime Hg(II) levels occurred frequently and exceeded rural background levels (generally below 10 ppqv) on 26 of 29 days in the summer and 8 of 15 days in the winter. Hg(II) enhancements were accompanied by strong depletions of Hg(0), down to 22 ppqv, which is below 10% of the global tropospheric background concentration, resulting in strong inverse correlations between the two (Fig. 1c), providing clear evidence for direct atmospheric conversion of Hg(0) to Hg(II). Most Hg(II) occurred in gaseous form, with only minor contributions of Hg(II) bound to particulates.

Hg(II) production and Hg(0) depletion temporally coincided with high BrO levels and depletion of O₃ (Fig. 1b and 2a), with high-resolution temporal data (5 min) demonstrating exact alignment of Hg(0) and O₃ depletions (Fig. 2b) and indicating that Hg(0) depletion and O₃ destruction were highly related. Observed enhancements of BrO and corresponding O₃ depletions agree with well-characterized intensive reactive bromine chemistry that occurs in the local Dead Sea atmosphere and causes significant catalytic destruction of O₃ first described here outside the high latitudes^{7,8,17}. The 'bromine explosion' mechanism¹⁸, induced by the high bromide level and low pH of the Dead Sea water, has been suggested as a key process for production of atmospheric BrO (refs 8,19). Observed oxidation of Hg(0) to Hg(II), in the presence of high BrO levels and O₃ destruction, shows all characteristics of AMDE previously only described in the high latitudes, and provides evidence of strong temperate-zone AMDE on an almost daily basis.

We modelled temporal patterns of halogen species, ozone and Hg(0) under typical summertime conditions (7 June 2009) using a heterogeneous chemical box model (MECCA; ref. 20), which accounts for 204 gas-phase, 292 aqueous-phase and 275 heterogeneous reactions, including 53 reactions involving mercury (Supplementary Section). When the full available bromine chemistry was implemented in the model (BASE scenario; Fig. 3a), it accurately simulated corresponding Hg(0) and O₃ depletions during the build-up of reactive bromine, which at the Dead Sea generally occurs near midday and in the afternoon^{8,17}. Sensitivity analyses using stepwise elimination of bromine reactions from the BASE scenario showed that using only BrO_x (=Br + BrO; named 'only BrO_x' in Fig. 3b) as oxidants for mercury can account for most of the observed AMDE. The use of atomic Br alone ('only Br'), a compound not directly measured, showed similar Hg(0) depletion to BrO_x, indicating that the effect of Br predominates over BrO (Fig. 3b). Model results also indicate that iodine species, which at the Dead Sea have been measured as iodine oxide (IO)

¹Division of Atmospheric Sciences, Desert Research Institute, 2215 Raggio Parkway, Reno, Nevada, 89512, USA, ²The Institute of Earth Sciences, The Hebrew University, Jerusalem 91904, Israel, ³Department of Atmospheric Chemistry, Max-Planck-Institute for Chemistry, Mainz 55128, Germany.

*e-mail: daniel.obrist@dri.edu.

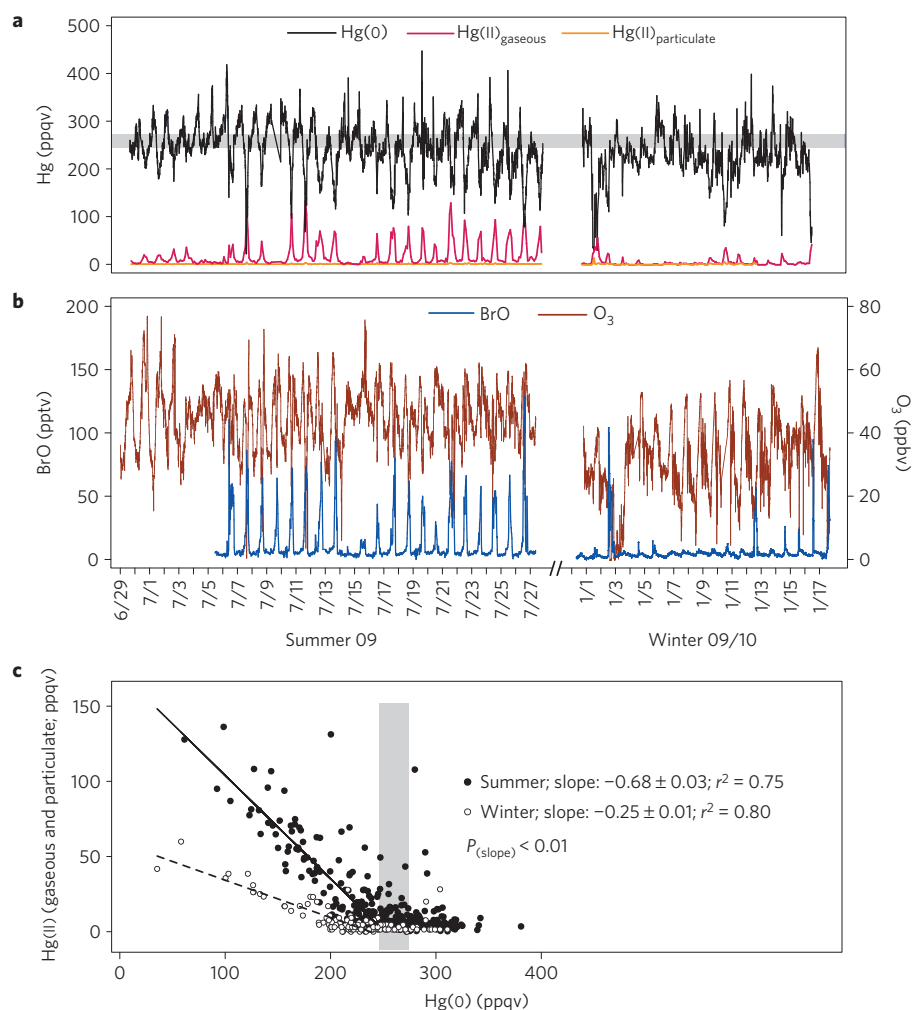


Figure 1 | Concentrations of mercury, BrO and O₃ during measurements. **a**, Time series of mercury, separated into Hg(0), Hg(II)_{gaseous} and Hg(II)_{particulate}. The tropospheric background of Hg(0) (245–275 ppqv) is marked as the shaded area. The time resolution for measurements is 5 min for Hg(0) and 2 h for Hg(II). **b**, BrO and O₃, with time resolutions of 15 min (BrO) and 5 min (O₃). **c**, Scatter plots and slopes (and standard errors) of linear regressions between Hg(II) (combined gaseous and particulate bound) and Hg(0) during conversion (that is, at Hg(0) below 245 ppqv). Summer data are filled symbols and winter data are open symbols.

up to 10 pptv (ref. 21), and chlorine species are unlikely efficient oxidants for mercury at the Dead Sea as evident by their low relative contributions to Hg(0) depletion (Supplementary Fig. S1). Iodine species seem to be inactive at high BrO_x levels on the basis of observations that BrO peaks only in the absence, or at low levels, of IO (ref. 21), and the role of chlorine species is considered less significant in the region owing to the high bromide to chloride ratio of the Dead Sea water. The box-model approach well represents chemical pathways, but meteorological conditions are parameterized only on the basis of typical conditions; as the chemical fate of atmospheric mercury is expected to respond to changes in meteorological conditions, it should be noted that the sensitivity runs are intended as qualitative analyses.

Both the frequency and magnitude of high Hg(II) levels were much more pronounced during summer than winter (Fig. 1), which can be explained in part by higher summer BrO levels. Concentrations of Hg(II), however, were also higher in summer at equivalent BrO levels, which we attribute to enhanced deposition and scavenging of Hg(II) in winter. Evidence for such immediate and substantial losses of converted Hg(II) is seen in a lack of mass balance between Hg(0) and Hg(II) (Fig. 1c), with Hg(II) accounting for 68% of depleted Hg(0) in summer but only for 25% in winter. Lack of mass balance between Hg(0) and Hg(II) during polar AMDE is attributed

to increased surface deposition of atmospheric mercury⁴. Most scavenged Hg(II) probably would not be detected by our system owing to a particulate-size cutoff (by a 2.5 μm impactor) smaller than many sea-salt aerosols. Possible reasons for higher mass losses, and hence likely higher deposition and scavenging losses, during wintertime AMDE may include higher presence of sea-salt aerosols—considered the main Hg(II) sink in the marine boundary layer²²—and higher humidity, which seems to reduce build-up of Hg(II) (ref. 23). The combined effects of efficient oxidation, dry conditions, low wind speeds and hence low sea-salt aerosol production in the Dead Sea summer may have enabled formation of some of the highest Hg(II) levels observed in the Earth's atmosphere.

Near-complete (that is, up to 90%) conversion of Hg(0) to Hg(II) by BrO_x in the warm Dead Sea atmosphere was unexpected, given that the kinetics are highly temperature dependent: specifically, thermal back-dissociation of HgBr—a crucial rate constant that is more than two orders of magnitude faster under mid-summer Dead Sea conditions compared with cold Arctic temperatures²⁴—should impede AMDE under warm conditions. A sensitivity analysis (Fig. 3c) using typical polar and Dead Sea winter and summer temperatures (~−33, 22 and 37 °C) confirms this temperature penalty under the chemical conditions of the Dead Sea. Both observations and model outputs, however, show that, in spite of

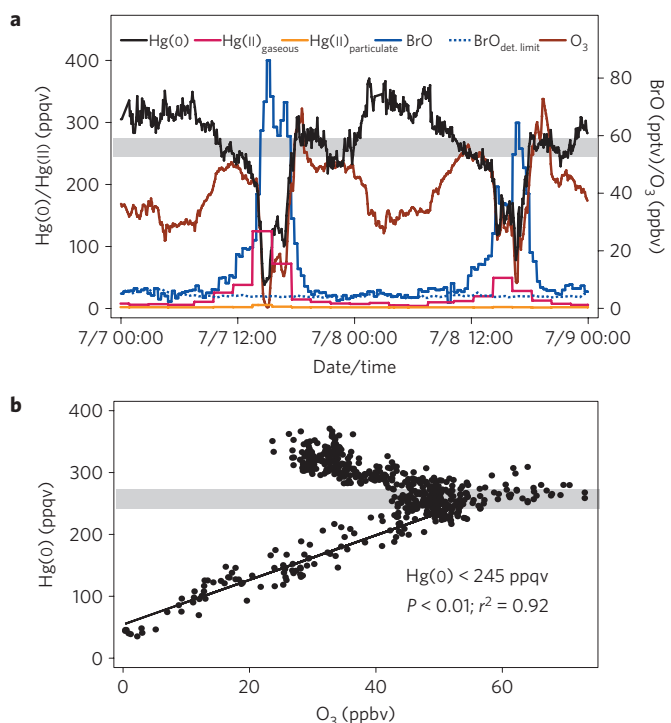


Figure 2 | Detailed mercury, BrO and O₃ patterns shown for two days with strong Hg(0) to Hg(II) conversions. **a**, Concentrations of Hg(0) (5 min resolution), Hg(II)_{gaseous} and Hg(II)_{particulate} (2 h resolutions), BrO (15 min resolution) and O₃ (5 min resolution) for 7 and 8 June 2009. The shaded area represents the global background Hg(0) concentration. The BrO detection limit is shown as a dotted line. **b**, Scatter plot between O₃ and Hg(0) and linear regression below global background Hg(0) levels (that is, during depletions) for the two days. Concentrations above global background Hg(0) represent mainly concentration enhancements in the nocturnal boundary layer and corresponding O₃ deposition.

this temperature penalty, almost complete AMDE can occur in the natural temperate atmosphere, even at temperatures up to 45 °C.

Hg(0) to Hg(II) conversion by no means solely occurred under atypically high BrO levels, however. We calculated Hg(II) production rates (that is, $\Delta\text{Hg(II)}/\Delta t$) during early daytime Hg(II) enhancements, and graphed production rates as a function of respective BrO levels (Fig. 4). Low BrO detection limits of the LP-DOAS system (as low as <2 pptv with a median value of 3.4 pptv; Supplementary Fig. S2) and time-extended measurements enabled us to assess Hg(II) production at BrO levels below 10 pptv. Hg(II) production rates were initiated at low BrO levels, as low as 4–6 pptv, in both winter and summer. Linear regressions between $\Delta\text{Hg(II)}/\Delta t$ and BrO using combined winter and summer data show an intercept of $\Delta\text{Hg(II)}/\Delta t$ at ~ 4 pptv BrO, and an increase in $\Delta\text{Hg(II)}/\Delta t$ of ~ 1 ppqv h⁻¹ per pptv BrO. The above BrO level (~ 4 pptv) for which Hg(II) production is first observed is conservative, because we used the maximum BrO levels (15 min time resolution) measured during the respective 2 h Hg(II) production intervals for this analysis. Low levels of atmospheric BrO (average peak daytime values ~ 2.8 pptv, with a maximum of 5.6 pptv) have been measured and may be ubiquitous over oceans in the mid-latitudes and tropics^{15,16,25,26}. Hence, BrO_x-induced Hg(II) production may be widespread and frequent across the global marine boundary layer. This notion is supported by previous partial Hg(0) depletions measured at the Dead Sea²⁷, observations of daytime Hg(II) enhancements in the remote marine boundary layer^{28,29}—although not necessarily along the coasts³⁰—and box model simulations²². Our study provides the first direct observation

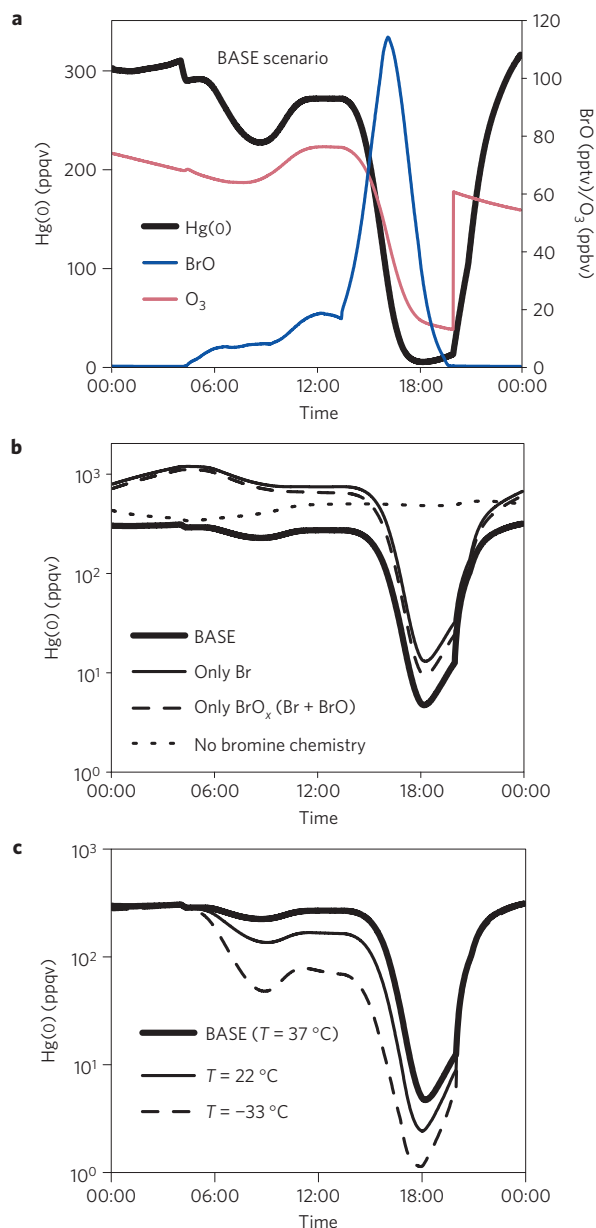


Figure 3 | Simulations using a heterogeneous chemical box model (MECCA).

a, Simulation of Hg(0), BrO and O₃ for typical summer conditions. This BASE scenario includes full reactive bromine chemistry. **b**, Sensitivity analyses of Hg(0) depletions using BASE conditions (same as **a**), elimination of bromine–mercury interactions (no bromine chemistry) and mercury oxidation by Br and BrO_x (Br + BrO) only. **c**, Sensitivity analysis of the effect of air temperatures under typical Dead Sea conditions. The analysis shows decreased efficiency of AMDE under warm summer temperatures (BASE; 37 °C) compared with typical wintertime (for example, 22 °C) and polar temperatures (–33 °C).

that Hg(0) to Hg(II) conversion by BrO_x occurs with high efficiency under temperate conditions, even at low BrO levels such as observed over the Earth's oceans.

Frequent atmospheric conversion of Hg(0) to Hg(II) shows that production of high Hg(II) levels is not limited to the cold high latitudes but is matched in both magnitude and frequency at the temperate-zone Dead Sea. Efficient mercury oxidation under warm conditions up to 45 °C and very low thresholds of BrO_x needed to initiate oxidation suggest that this mechanism is important across the temperate and tropical marine boundary layer where low levels

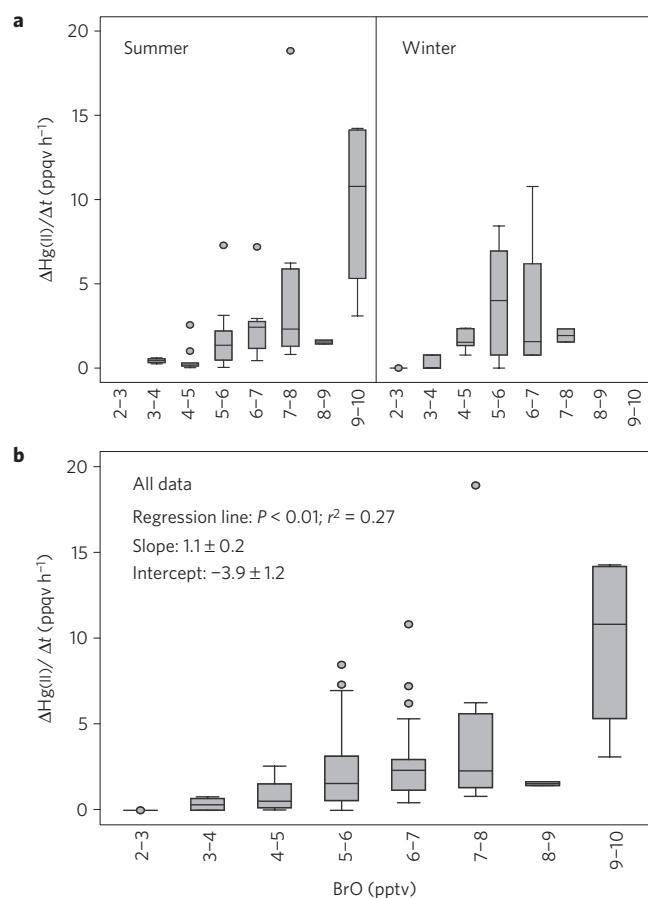


Figure 4 | Box-plot analyses of Hg(II) production rates ($\Delta\text{Hg(II)}/\Delta t$) as a function of BrO levels during early daytime Hg(II) formation. **a, Box plots showing 25th, 50th and 75th percentiles (horizontal bars), and 1.5 interquartile ranges (error bars) of Hg(II) production rates for bins of measured BrO concentrations for summer and winter measurements. **b**, Corresponding box plots of Hg(II) production rates for all measurements combined, including slope and intercept (plus standard errors) of linear regression between $\Delta\text{Hg(II)}/\Delta t$ and BrO.**

of gaseous BrO are observed. Given that 80–90% of Hg(II) formed in the marine boundary layer enters the oceans²², bromine-driven Hg(II) formation could be a main source of atmospheric mercury to oceans, where it can be subject to methylation³¹ and contribute to human mercury exposure by consumption of seafood³².

Methods

We made measurements at Ein Bokek, Israel (latitude 31.20° N, longitude 35.37° E), on the shore of the Dead Sea. Instrumentation inlets were situated on the top-floor balcony of a hotel 25 m inland and 20 m above water level. We made Hg(0) and Hg(II) measurements from 29 June to 28 July 2009 and from 29 December to 17 January 2010 using model 2537 vapour-phase mercury analysers and model 1130 and model 1135 mercury speciation units (Tekran, Toronto, Canada). Tekran 1130 and 1135 units were configured to collect 1 h composite gaseous and particulate-bound Hg(II) samples followed by 1 h desorption and analysis processes. Total instrument sampling flows were set to 9.5 l min⁻¹ at STP conditions (273.15 K, 1013.25 mbar), resulting in an actual volume flow of ~10 l min⁻¹ at the temperature and pressure conditions of the Dead Sea and providing a 2.5- μm -particle-size cutoff through an impactor. We measured BrO and NO₂ using the LP-DOAS technique (model HMT DOAS Measuring System, Hoffmann Messtechnik, Rauensberg, Germany). We placed the DOAS reflector mirror on an earth mound lining an evaporation pond, resulting in an 11.8 km light path travelling directly over Dead Sea water to the west. Detection limits for BrO were dependent on alignments and visibility, with the lowest value below 2 pptv and a median detection limit of 3.4 pptv (see Supplementary Fig. S2). Ozone was monitored using the ultraviolet-absorption method (TEII, model 49C), and other trace-gas measurements included NO–NO_x (TEII, model 42i), CO (TEII,

model 48i) and SO₂ (TEII, model 43C; all Thermo Environment Instrument Incorporated, Waltham, USA). In spite of different spatial scales of measurements (for example, LP-DOAS with 11.8 km absorption path length and average height between hotel elevation and sea surface level) and point measurements on the hotel balcony (20 m above sea level; including all mercury measurements and other trace gases), these measurements compared well as assessed by comparison of O₃ concentrations quantified by both LP-DOAS and a monitor (Supplementary Fig. S3). In addition, meteorological parameters (wind speed and direction, temperature, humidity, barometric pressure and solar radiation) were measured using Met-One instrumentation.

We carried out box simulations using the MECCA (ref. 20) model with 204 gas-phase, 292 aqueous-phase and 275 heterogeneous reactions. Several simulations and sensitivity analyses were carried out, starting with a BASE scenario, which included the full bromine chemistry available in the model. Simulations were carried out for typical summer conditions with temperature and RH averaging 37 °C and 37%, and details of the model runs are given in Supplementary Methods. For sensitivity analysis, the BASE case simulations were repeated after removal of all interactions of bromine compounds with mercury ('no bromine' case). Simulations were then carried out by inclusion of Br as the only oxidant for mercury ('only Br' case) and inclusion of Br + BrO as sole oxidants for mercury ('only BrO_x' case). Temperature-sensitivity analyses were carried out by implementation of different temperature regimes (that is, 37 °C for the BASE case, 22 °C for wintertime conditions and -33 °C for polar conditions) for all mercury-containing, gas-phase reactions. Heterogeneous-phase reactions did not show sensitivity to temperature changes, and all other environmental and chemical parameters remained as measured during typical summertime conditions.

Received 19 May 2010; accepted 22 October 2010;
published online 28 November 2010

References

- Fitzgerald, W. F., Engstrom, D. R., Mason, R. P. & Nater, E. A. The case for atmospheric mercury contamination in remote areas. *Environ. Sci. Technol.* **32**, 1–7 (1998).
- Mason, R. P. & Sheu, G.-R. Role of the ocean in the global mercury cycle. *Global Biogeochem. Cycles* **16**, 1093 (2002).
- Schroeder, W. H. *et al.* Arctic springtime depletion of mercury. *Nature* **394**, 331–332 (1998).
- Steffen, A. *et al.* A synthesis of atmospheric mercury depletion event chemistry in the atmosphere and snow. *Atmos. Chem. Phys.* **8**, 1445–1482 (2008).
- McConnell, J. C. *et al.* Photochemical bromine production implicated in Arctic boundary-layer ozone depletion. *Nature* **355**, 150–152 (1992).
- Fan, S.-M. & Jacob, D. J. Surface ozone depletion in Arctic spring sustained by bromine reactions on aerosols. *Nature* **359**, 522–524 (1992).
- Hebestreit, K. *et al.* DOAS measurements of tropospheric bromine oxide in mid-latitudes. *Science* **283**, 55–57 (1999).
- Matveev, V. *et al.* Bromine oxide–ozone interaction over the Dead Sea. *J. Geophys. Res. Atmos.* **106**, 10375–10387 (2001).
- Lu, J. Y. *et al.* Magnification of atmospheric mercury deposition to polar regions in springtime: The link to tropospheric ozone depletion chemistry. *Geophys. Res. Lett.* **28**, 3219–3222 (2001).
- Lindberg, S. E. *et al.* Formation of reactive gaseous mercury in the arctic: Evidence of oxidation of Hg⁰ to gas-phase Hg-II compounds after arctic sunrise. *Water Air Soil Pollut.* **1**, 295–302 (2001).
- Ariya, P. A. *et al.* The arctic: A sink for mercury. *Tellus Ser. B-Chem. Phys. Meteorol.* **56**, 397–403 (2004).
- Skov, H. *et al.* Fate of elemental mercury in the Arctic during atmospheric mercury depletion episodes and the load of atmospheric mercury to the Arctic. *Environ. Sci. Technol.* **38**, 2373–2382 (2004).
- Brooks, S. B. *et al.* The mass balance of mercury in the springtime arctic environment. *Geophys. Res. Lett.* **33**, L13812 (2006).
- Bottenheim, J. W., Gallant, A. G. & Brice, K. A. Measurements of NO_y species and O₃ at 82-degree N latitude. *Geophys. Res. Lett.* **13**, 113–116 (1986).
- Saiz-Lopez, A., Plane, J. M. C. & Shillito, J. A. Bromine oxide in the mid-latitude marine boundary layer. *Geophys. Res. Lett.* **31**, L03111 (2004).
- Read, K. A. *et al.* Extensive halogen-mediated ozone destruction over the tropical Atlantic Ocean. *Nature* **453**, 1232–1235 (2008).
- Tas, E. *et al.* Frequency and extent of bromine oxide formation over the Dead Sea. *J. Geophys. Res. Atmos.* **110**, D11304 (2005).
- Vogt, R., Crutzen, P. J. & Sander, R. A mechanism for halogen release from sea-salt aerosol in the remote marine boundary layer. *Nature* **383**, 327–330 (1996).
- Tas, E. *et al.* Measurement-based modeling of bromine chemistry in the boundary layer: 1. Bromine chemistry at the Dead Sea. *Atmos. Chem. Phys.* **6**, 5589–5604 (2006).
- Sander, R., Kerkweg, A., Jockel, P. & Lelieveld, J. Technical note: The new comprehensive atmospheric chemistry module MECCA. *Atmos. Chem. Phys.* **5**, 445–450 (2005).

21. Zingler, J. & Platt, U. Iodine oxide in the Dead Sea Valley: Evidence for inorganic sources of boundary layer IO. *J. Geophys. Res. Atmos.* **110**, D07307 (2005).
22. Holmes, C. D., Jacob, D. J., Mason, R. P. & Jaffe, D. A. Sources and deposition of reactive gaseous mercury in the marine atmosphere. *Atmos. Environ.* **43**, 2278–2285 (2009).
23. Fain, X. *et al.* High levels of reactive gaseous mercury observed at a high elevation research laboratory in the Rocky Mountains. *Atmos. Chem. Phys.* **9**, 8049–8060 (2009).
24. Goodsite, M. E. & Plane, J. M. C. A theoretical study of the oxidation of Hg⁰ to HgBr₂ in the troposphere. *Environ. Sci. Technol.* **38**, 1772–1776 (2004).
25. Sander, R. *et al.* Inorganic bromine in the marine boundary layer: A critical review. *Atmos. Chem. Phys.* **3**, 1301–1336 (2003).
26. Lee, J. D. *et al.* Reactive halogens in the marine boundary layer (RHaMBLe): The tropical North Atlantic experiments. *Atmos. Chem. Phys.* **10**, 1031–1055 (2010).
27. Peleg, M. *et al.* Mercury depletion events in the troposphere in mid-latitudes at the Dead Sea, Israel. *Environ. Sci. Technol.* **41**, 7280–7285 (2007).
28. Sprovieri, F., Pirrone, N., Garfield, K. & Sommar, J. Mercury speciation in the marine boundary layer along a 6,000 km cruise path around the Mediterranean Sea. *Atmos. Environ.* **37**, 563–571 (2003).
29. Laurier, F. J. G., Mason, R. P., Whalin, L. & Kato, S. Reactive gaseous mercury formation in the North Pacific Ocean's marine boundary layer: A potential role of halogen chemistry. *J. Geophys. Res. Atmos.* **108**, 4529 (2003).
30. Malcolm, E. G., Keeler, G. J. & Landis, M. S. The effects of the coastal environment on the atmospheric mercury cycle. *J. Geophys. Res. Atmos.* **108**, 4357 (2003).
31. Sunderland, E. M. *et al.* Mercury sources, distribution, and bioavailability in the North Pacific Ocean: Insights from data and models. *Glob. Biogeochem. Cycles* **23**, GB2010 (2009).
32. Sunderland, E. M. Mercury exposure from domestic and imported estuarine and marine fish in the US seafood market. *Environ. Health Perspect.* **115**, 235–242 (2007).

Acknowledgements

We thank R. Kreidberg for editorial assistance; the Dead Sea Works for site logistics; J. Zingler, J. Lenvant and U. Corsmeier for meteorological data; R. Sander for use of the MECCA model; L. Wable for graphical support and J. A. Arnone, S. Lindberg and J. McConnell for critical reviews on an earlier manuscript. The study was funded by the US National Science Foundation (no 0813690 to D.O. and M.L.), and has benefited from a US Environmental Protection Agency Star-to-Achieve grant (R833378).

Author contributions

D.O. and M.L. led the study, including proposal writing, project coordination, data interpretation and manuscript preparation; D.O., M.P., V.M., X.F. and D.A. were directly involved with field measurements at the Dead Sea, data collection and data analysis; E.T. carried out modelling and interpretation of these results. All authors discussed the results and contributed to the manuscript.

Additional information

The authors declare no competing financial interests. Supplementary information accompanies this paper on www.nature.com/naturegeoscience. Reprints and permissions information is available online at <http://npg.nature.com/reprintsandpermissions>. Correspondence and requests for materials should be addressed to D.O.